Dielectric Relaxation of Liquid Crystalline Cyanoethylated *O*-(2,3-Dihydroxypropyl)cellulose

Takaya Sato, Yoshinobu Tsujii, Yasuo Kita, Takeshi Fukuda, and Takeaki Miyamoto*

Institute for Chemical Research, Kyoto University, Uji, Kyoto 611, Japan

Received October 29, 1990; Revised Manuscript Received March 27, 1991

ABSTRACT: Studied was the dielectric relaxational behavior of fully cyanoethylated *O*-(2,3-dihydroxypropyl)-cellulose, which is a liquid crystalline polymer characterized by a low glass transition temperature T_g and an extremely high dielectric constant. Three relaxations, designated β, α, and α', were observed for all three derivatives studied, independently of the molar substitution of the dihydroxypropyl unit and the anisotropic–isotropic phase transition temperature. The β relaxation, active essentially below T_g, is assignable to local motions in the side chain. The α and α' relaxations are active above T_g, the former appearing at lower temperatures than, and having an activation energy about twice as large as, the latter. Both of these relaxations are assigned to main-chain motions of different modes that set in at T_g. It is suggested that the α' mode is associated with a rotational motion of the whole side chain about the main-chain axis, while the α mode is associated with other center of mass motions of the main and side chains. Perhaps the semirigidity of the cellulose backbone is responsible for the appearance of these two clearly separated relaxation processes above T_g. The liquid crystalline order of molecules has no dielectric relevance to the dielectric relaxations. The dielectric results were supplemented and confirmed in part by dynamic viscoelastic measurements of the same system. The viscoelastic properties reflected, to some extent, the liquid crystalline state of the system.

Introduction

Dielectric relaxation processes of liquid crystalline (LC) polymers were studied in many recent publications,[1-14] most of which dealt with comblike polymers comprising a flexible main chain and mesogenic side chains.[1-11] Relatively few of them were concerned with main-chain LC polymers like polyesters.[12-14]

Polysaccharides and their derivatives are also among polymers that have been studied by the dielectric method.[15-24] Dielectric measurements of this class of polymers, however, were limited mostly to temperatures below the glass transition T_g, where only local side-chain motions were observed. Measurements at higher temperatures were increasingly difficult because of often destructive contributions to conductance from ionic impurities, which were difficult to remove perfectly. For this reason, the main-chain motions in polysaccharide systems have been studied exclusively by viscoelastic measurements.[24-29]

Cellulose is a semirigid unmeltable polymer, whose T_g and plastization temperature can be drastically lowered by introducing an appropriate side chain, most effectively in a chemically disordered fashion. Such cellulose derivatives often form a thermotropic LC phase.[30-33] Except for one known case,[34] cellulosic mesophases are cholesterics (or nematics), which originate essentially from the semirigidity and chirality of the main chain.[35]

Fully cyanoethylated *O*-(2,3-dihydroxypropyl)cellulose (DHPC) is a chemically disordered LC polymer which is characterized by low T_g, a wide temperature range of mesophase, and an extraordinarily high dielectric constant.[36] Extensive purification of this polymer has enabled us to carry out dielectric measurements up to high enough temperatures to observe the main-chain motions. This paper reports the first observation of two dielectric relaxation processes *above* T_g for a polysaccharide system and for a semirigid, main-chain LC polymer.

Experimental Section

Polymer Samples. Four fully cyanoethylated DHPC samples (Figure 1) were used in this study. These samples were prepared

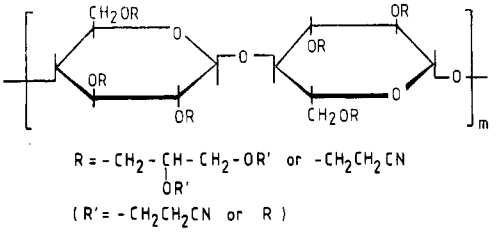

Figure 1. Chemical structure of cyanoethylated *O*-(2,3-dihydroxypropyl)cellulose (CN-DHPC).

starting with a degenerated cellulose having a number-average degree of polymerization of about 210. Their molecular characteristics and thermal properties are listed in Table I. Details have been reported elsewhere.[36] To remove ionic and other low molecular weight impurities, an acetone solution of each sample was dialyzed against deionized water for 10 days. During the course of dialysis, the polymer, which was insoluble in water, gradually precipitated out from the solution. After this process was repeated three times, the polymer was recovered and dried in vacuo at 80 °C for 3 days. It was vacuum-dried again prior to each measurement.

Dielectric Measurements. Dielectric measurements were conducted on a Hewlett-Packard Model 4284A precision LCR meter at about 100 different temperatures ranging from 150 to 400 K (temperature interval 2.5 K) and at 50 different frequencies ranging from 20 Hz to 1 MHz for each temperature. Temperature was controlled with an Ohkura EC-7 controller and measured with a copper vs constantan thermocouple along with a Keithley 196 digital multimeter system. The whole system was fully controlled with an Epson Model PC-286VE personal computer.

A three-terminal dielectric cell specially designed for fluid polymers was employed (Figure 2). It consisted of a hemispheroid–cylindrical electrode A, which was guarded by a guard electrode C, and an unguarded electrode B placed concentrically with electrode A, with an exact gap of 500 μm between them. The unguarded portion of this gap formed a (net) sample room. All electrodes were made of stainless steel SUS 303. This three-electrode construction permitted the elimination of possible effects of sample overloading and electric fringe. The cell capacity was measured to be 8.50 pF, which reasonably agreed with the value of 8.34 pF expected from the sample cell dimensions (10-mm o.d., 15-mm height, and 0.50-mm width). To load a polymer sample, the upper portion of the cell including electrode A was

0024-9297/91/2224-4691$02.50/0

Table I
Molecular and Thermal Characteristics of CN-DHPC Samples

sample code	$10^{-4}M_{GPC}$[a]	MS[b]	T_g,[c] °C	T_s,[d] °C	T_i,[e] °C
DH-2-CN	4.0	2.25	−27	30	130
DH-4-CN	4.5	4.18	−28	17	90
DH-4-CN′	4.5	3.45	−42	23	100
DH-8-CN	3.7	8.45	−40	16	

[a] Value before cyanoethylation, estimated by a poly(ethylene oxide)-calibrated GPC analysis. [b] Molar substitution of DHPC unit. [c] Glass transition temperature. [d] See text. [e] Isotropization temperature.

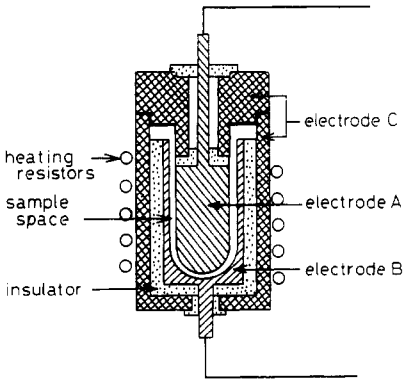

Figure 2. Schematic representation of the dielectric cell.

removed, and an appropriate amount of the polymer was placed on the bottom of electrode B while the system was heated to 50 °C to make the polymer fluid enough. Then the upper portion of the cell was slowly inserted by applying some pressure so that the molten polymer filled the cell. The system was then cooled, at an approximate rate of 0.5 K/min, to 150 K, where the measurements were started. During the cooling process, the permittivity and conductance sometimes showed an abrupt, discontinuous change, indicating an anomaly in the sample or at the sample–electrode interface. Whenever this happened, the sample was replaced and the above-mentioned process was repeated.

Dynamic Viscoelastic Measurements. Viscoelastic measurements were made on a Rheometrics RDS-II dynamic spectrometer installed with a cone plate (25-mm diameter and 0.1-rad cone angle). The strain amplitude, i.e., the ratio of oscillation amplitude to the cone angle, was unity. Use of a Rheometrics RSA-II solid analyzer was also made for solid or liquid crystalline specimens. All measurements were made under a nitrogen atmosphere.

Results

Dielectric measurements were made for the three polymer samples coded DH-2-CN, DH-4-CN, and DH-8-CN. Analyses by differential scanning calorimetry (DSC) showed that these polymers have T_g around −30 or −40 °C. The first two polymers exhibit liquid crystallinity even at room temperature. Observations under a polarization optical microscope revealed that these polymers become anisotropic–isotropic biphasic at 60–70 °C or above and entirely cease to be birefringent at about 130 °C for DH-2-CN and at about 90 °C for DH-4-CN. These temperatures will be denoted T_i (Table I). The DSC analyses did not clearly show the anisotropic–isotropic phase transition of these polymers, as is usually the case with polymers having a broad transition region.[37] The DSC thermograms of the present polymers, however, indicated another kind of "transition" at a lower temperature. An example is given in Figure 3, where the transition, tentatively denoted T_s, may look something like a (secondary) glass transition rather than a first-order phase transition. An X-ray diffraction analysis gave no indication of (solid) crystallinity in the temperature region between T_g and T_s. Qualitatively, the polymer below T_s is rather hard and rubbery, while above T_s it is softer, is easier to be sheared, and appears to be more birefringent. Sample DH-8-CN, which shows no apparent liquid crystallinity at room temperature, also exhibits this characteristic temperature T_s. One of the motives of the present work was to study the nature of this transition T_s by dielectric and viscoelastic methods.

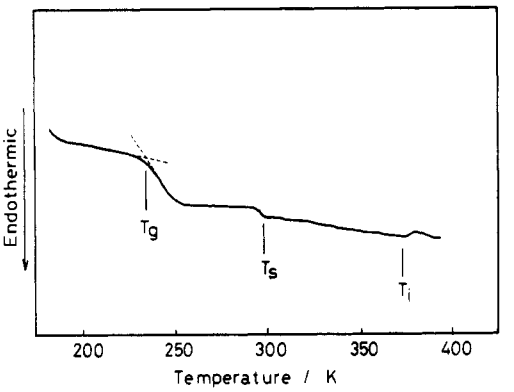

Figure 3. DSC thermogram for sample DH-4-CN′.

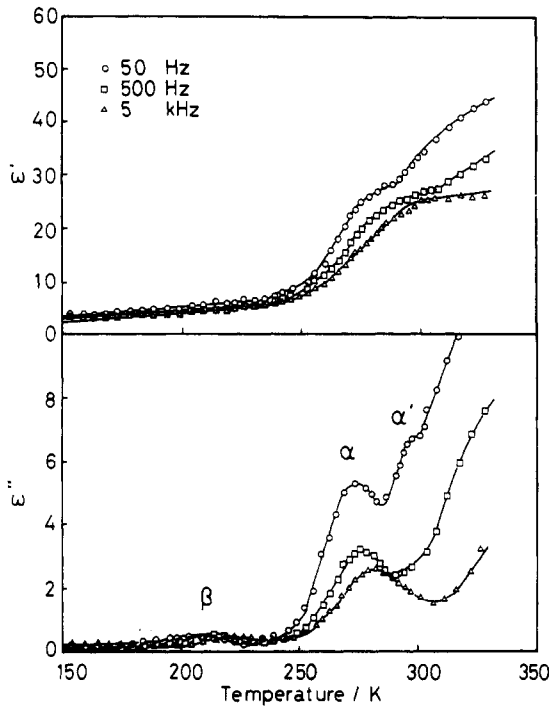

Figure 4. Temperature dependence of dielectric constant ϵ' and dielectric loss ϵ'' for DH-2-CN.

Dielectric Measurements. Figures 4–6 show the temperature dependence of dielectric constant ϵ' and dielectric loss ϵ'' of the three samples measured at three representative frequencies 50 and 500 Hz and 5 kHz. The loss factor curves for sample DH-4-CN (Figure 5) clearly show three relaxations, which we shall denote β, α, and α' in order of increasing temperature. For each relaxation, the temperature at which ϵ'' is maximum increases with increasing frequency f. The other two samples show similar behavior, even though their α' relaxations are less clearly visible because of the steep rise of the curves at higher temperatures, which is caused by ionic impurities (Figures 4 and 6).

Figure 7 compares the ϵ'' curves of the three samples measured at $f = 50$ Hz. The β relaxation appears at about

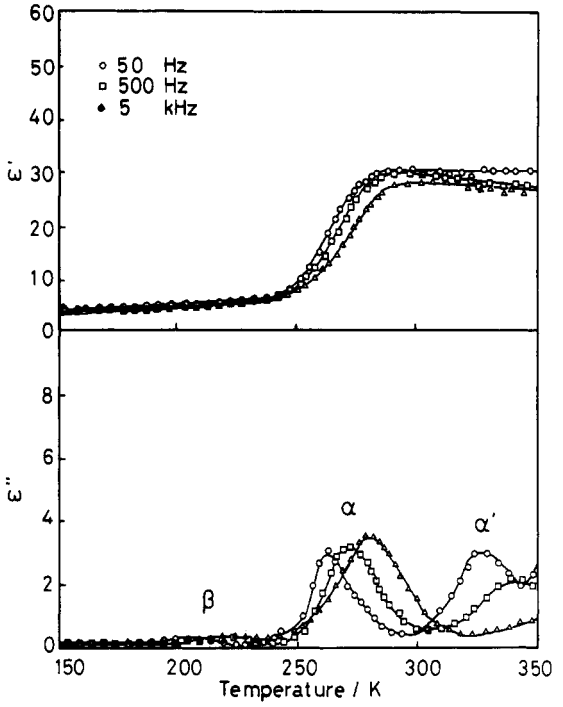

Figure 5. Temperature dependence of dielectric constant ϵ' and dielectric loss ϵ'' for DH-4-CN.

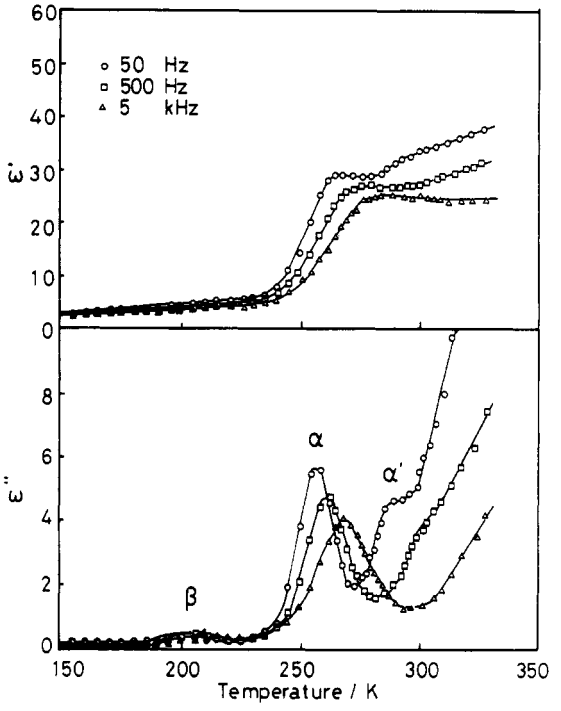

Figure 6. Temperature dependence of dielectric constant ϵ' and dielectric loss ϵ'' for DH-8-CN.

the same temperatures for all samples, while the α and α' relaxations appear at different temperatures for different samples.

Figure 8 shows the f dependence of ϵ' and ϵ'' for sample DH-4-CN measured at −50 (below T_g, Figure 8a), −10 (between T_g and T_s, Figure 8b), 36 (between T_s and T_i, Figure 8c), and 96 °C (above T_i, Figure 8d). Again, ionic impurities are responsible for the increase of ϵ' and ϵ'' at low frequencies (Figure 8d). In the present range of f, only the β relaxation is observed at −50 °C and the α relaxation becomes observable at −10 °C (about 18 °C above T_g). At 36 °C or above, the α' relaxation is observable. This relaxation is observed even at 96 °C,

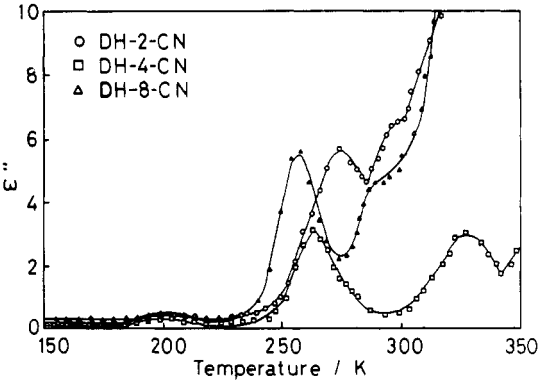

Figure 7. Temperature dependence of dielectric loss ϵ'' for DH-2-CN, DH-4-CN, and DH-8-CN (f = 50 Hz).

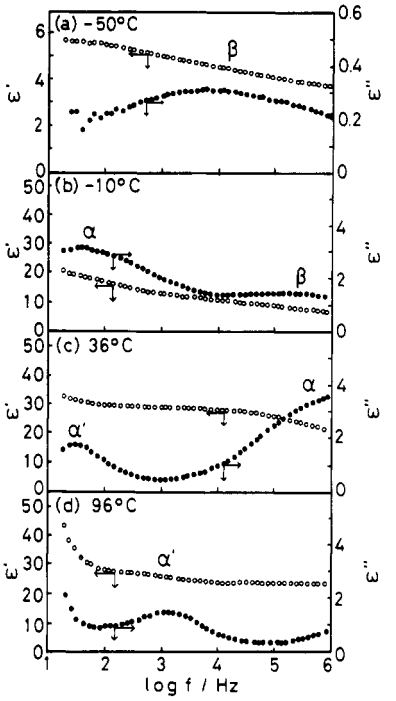

Figure 8. Frequency dependence of ϵ' and ϵ'' for DH-4-CN at various temperatures.

where the system is isotropic. It is also noted that sample DH-8-CN, which forms no LC phase, shows the α' relaxation (cf. Figure 6).

Figure 9 shows the Arrhenius plot of f_{max} for the three relaxations, where f_{max} is the frequency at which ϵ'' is maximum in the ϵ'' vs f curve. We see that the Arrhenius law is followed in all cases. The activation energies estimated from the figure are listed in Table II. They are nearly independent of samples, i.e., ca. 56 kJ/mol for β, ca. 146 kJ/mol for α, and ca. 72 kJ/mol for α'.

Master curves regarding the f dependence of ϵ' and ϵ'' for temperatures higher than T_g were constructed by taking 20 °C as a reference temperature. An example is given in Figure 10. As the figure shows, the data for different temperatures are apparently well superposable. However, we cannot expect a perfect superposability in a strict sense, because, as has been already shown, the α and α' relaxations are different in activation energy. Nevertheless, such master curves are practically useful for a comprehensive understanding of the relaxation process. We have analyzed the master curves by assuming that they consist of three components, i.e., the α and α' relaxations and the one appearing at the lowermost frequencies that is ascribed to low molecular weight impurities. Each component was

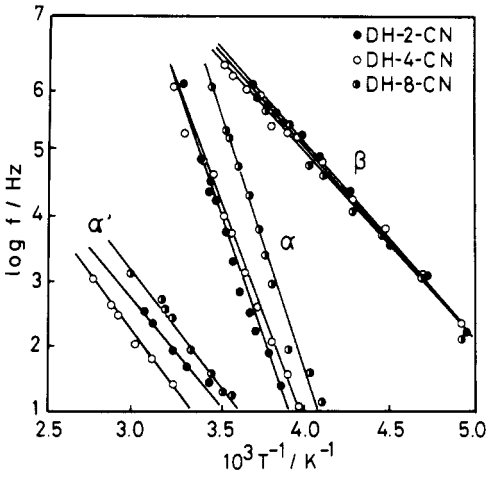

Figure 9. Plots of log f_{max} against T^{-1} for the β, α, and α' relaxations.

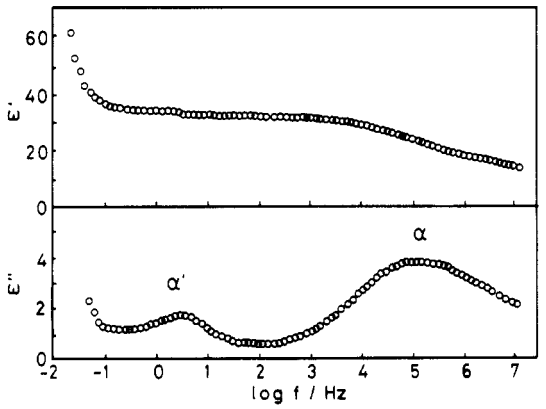

Figure 10. Master curves representing the frequency dependence of ϵ' and ϵ'' for DH-4-CN ($T > T_g$). Reference temperature, 20 °C.

Table II
Activation Energies for the Three Relaxation Processes

	activation energy, kJ/mol		
sample code	β	α	α'
DH-2-CN	57.8	147.5	68.8
DH-4-CN	54.9	142.7	73.1
DH-8-CN	56.6	148.7	72.7

assumed to be described by the Cole–Cole equation

$$\epsilon = \epsilon^* + \frac{\epsilon_s - \epsilon_\infty}{1 + (i\omega\tau_0)^b} \quad (1)$$

where ϵ^* is the complex dielectric constant, ω is the angular frequency ($\omega = 2\pi f$), τ_0 is the mean relaxation time, ϵ_s and ϵ_∞ are the dielectric constants in the low- and high-frequency limits, respectively, and b is a parameter characterizing the broadness of the relaxation time distribution. The experimental data were generally well fitted to this three-component Cole–Cole scheme. Values of the mean relaxation frequency f_0, the relaxation strength $\Delta\epsilon$, and b are listed in Table III, where

$$f_0 = 1/(2\pi\tau_0) \quad (2)$$

$$\Delta\epsilon = \epsilon_s - \epsilon_\infty \quad (3)$$

The shift factor a_T used for the construction of the master curves is plotted against inverse temperature in Figure 11. Clearly, there exists a temperature at which each curve changes its slope. We shall denote this temperature T_b. The slopes of the higher and lower temperature branches of each curve approximately agree with those of the Arrhenius curves for the α and α' relaxations, respectively, as one would expect. In view of the mentioned rigor-lacking nature of the master curve construction, it is difficult to define T_b in strict physical terms. Qualitatively, we may possibly mention that in the present frequency range we are predominantly observing the α relaxation at $T < T_b$ and the α' relaxation at $T > T_b$.

Viscoelastic Measurements. To confirm or supplement the dielectric data, dynamic viscoelastic measurements were made for sample DH-4-CN′, which is nearly equivalent to sample DH-4-CN. Figure 12 shows the temperature dependence of the shear storage and loss moduli (G' and G''), the tensile storage and loss moduli (E' and E''), and the loss tangent (tan $\delta = G''/G'$ or E''/E'). The angular frequency ω was kept at 1 rad/s. The shear experiments were possibly made for temperatures between 20 and 190 °C and the tensile experiments for temperatures between −140 and 100 °C. Thus, the temperature region from 20 to 100 °C was commonly covered by the two types of experiments. As Figure 12 shows, the shear and tensile data for this temperature region are consistent with each other, if we assume that $E/G \simeq 4$ instead of the theoretical ratio 3. This deviation is probably caused by an error in the determination of the sample dimensions for the tensile experiments, which were approximately measured as 1 mm × 10 mm × 20 mm. Clearly seen in the figure are only two relaxations, which will correspond to the dielectric β and α (or α'). The gradual increase of tan δ at around 80 or 90 °C may correspond to the anisotropic to isotropic phase transition.

Figure 13 shows the master curves for G' and G'' constructed with the data for 20 °C ≤ T ≤ 120 °C by taking 20 °C as a reference temperature. The data for T > 120 °C, where the system is isotropic, were not superposable on these curves. In Figure 11b, the relevant shift factor is compared with the dielectric a_T. The reasonable agreement of the two sets of a_T data will confirm consistency between the dielectric and viscoelastic experiments.

Discussion

β Relaxation. Of the three dielectric relaxations, the β relaxation appears at the lowest temperatures. The values of f_0, $\Delta\epsilon$, and b as well as the log f_{max} vs T^{-1} curve are nearly independent of sample (see Table III and Figure 9). Similar insensitivities of the β process to the side-chain chemistry have been reported for polymethacrylates.[38,39] The log f_{max} vs T^{-1} curves in Figure 9, if extrapolated to low frequencies, indicate that the β relaxation will be observed, for the frequency of ω = 1 rad/s or $f = (2\pi)^{-1}$ Hz, at a temperature as low as about −100 °C. This is confirmed by the viscoelastic data in Figure 12. This relaxation, appearing well below T_g for low frequencies, may be assigned to local motions in the side chains. It has a relatively small value of the Cole–Cole distribution parameter b, indicating a rather broad distribution of relaxation time. The high degree of chemical disorder in the side group substituents of these polymers may be responsible for the broad distribution in relaxation time. The temperature region and the activation energy for this relaxation approximately agree with those reported for cyanoethyl cellulose and assigned similarly.[15-17]

α Relaxation. Striking is the fact that our polymers show two dielectric relaxations above T_g, of which the α relaxation appears at lower temperatures and has an

Table III
Cole–Cole Parameters for the β, α, and α′ Relaxation Processes[a]

sample code	f_0, Hz			Δε			b		
	β	α	α′	β	α	α′	β	α	α′
DH-2-CN	1.3×10^5	7.2×10^4	2.3×10	5.0	15.0	18.0	0.56	0.39	0.73
DH-4-CN	1.3×10^5	1.0×10^5	4.3	3.9	17.7	4.5	0.44	0.45	0.70
DH-8-CN	1.5×10^5	4.6×10^6	5.1×10	4.2	18.5	13.0	0.48	0.46	0.72

[a] Values for 20 °C except for those for the β relaxation which is for −21 °C.

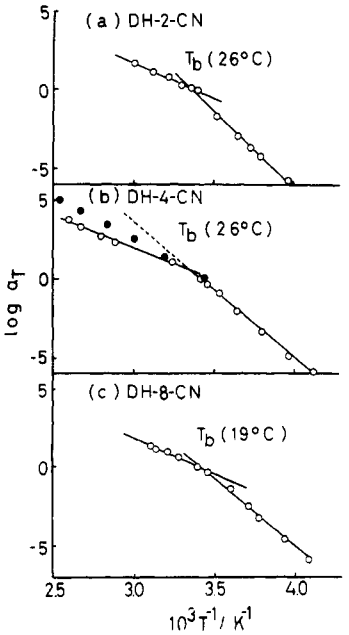

Figure 11. Dielectric shift factor a_T plotted against T^{-1} (open circles). The solid circles in (b) are relevant to the dynamic viscoelastic data for sample DH-4-CN′.

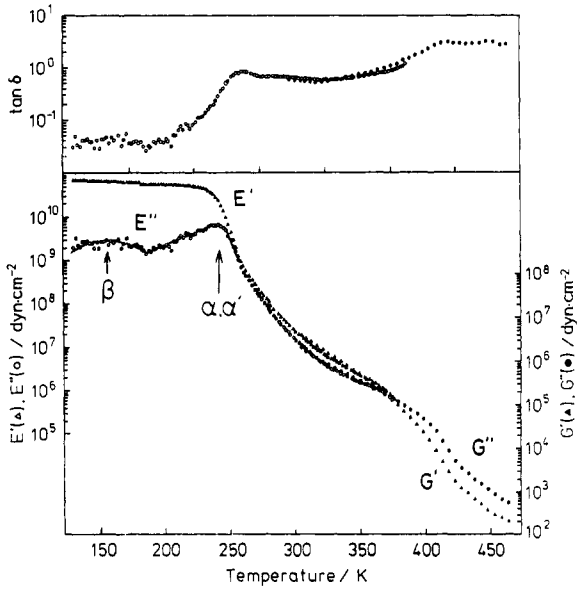

Figure 12. Temperature dependence of the tensile storage and loss moduli (E' and E''), shear storage and loss moduli (G' and G''), and the loss tangent (tan δ) for sample DH-4-CN′. $\omega = 1$ rad/s (see text for details).

activation energy about twice as large as that of the other, the α′ relaxation. In Figure 14, we have attempted to correct the log f_{max} vs T^{-1} curves in Figure 9 for the T_g differences among the samples by horizontally shifting the curves by an amount $c_T = T_{go}^{-1} - T_g^{-1}$, where T_{go} refers to the reference sample, DH-4-CN. With this correction, both the α and α′ sets of data roughly fall on a respective single curve. These "master" curves, if linearly extended

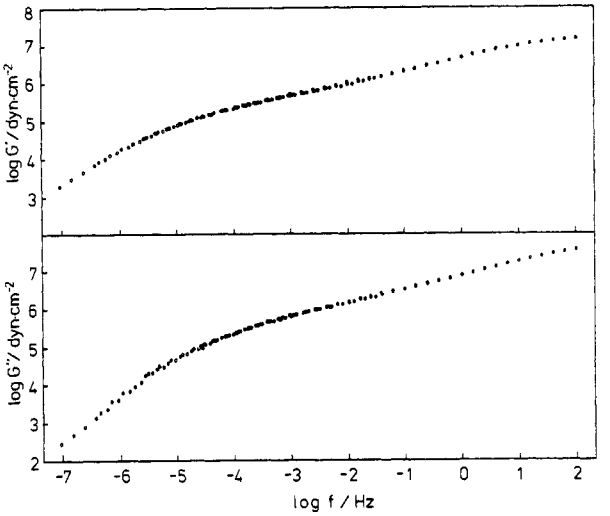

Figure 13. Master curves representing the frequency dependence of G' and G'' for sample DH-4-CN′ (20 °C < T < 120 °C). Reference temperature, 20 °C. The relevant shift factors are given in Figure 11b.

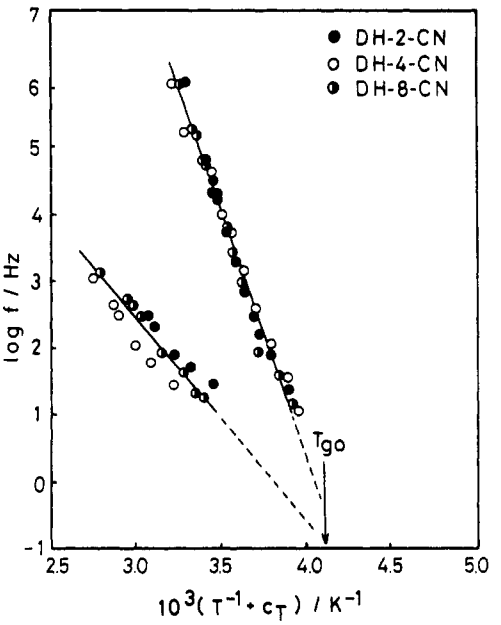

Figure 14. Plots of log f_{max} against $T^{-1} + c_T$ with $c_T = T_{go}^{-1} - T_g^{-1}$, where T_{go} refers to the reference sample, DH-4-CN.

to low frequencies, seem to intersect each other at a temperature close to T_g and at a frequency of about 10^{-1} Hz. This indicates, on the one hand, that both α and α′ are closely related to T_g and, on the other, that at very low frequencies the two relaxation spectra will superpose on each other. This latter expectation is confirmed again by the viscoelastic data in Figure 12, which show only one relaxation near T_g for $f = (2\pi)^{-1}$ Hz. We may conclude that both α and α′ are associated with main-chain motions of different modes that set in at the glass transition.

At the glass transition the centers of gravity of the side chains and the cellulose main chain become mobile. Dipole

reorientations associated with these motions will contribute to the α relaxation. A rather broad distribution of relaxation time is indicated by the Cole–Cole parameter b for this mode (Table III).

α' Relaxation. This relaxation is associated with a much slower motion. Since this relaxation is observable even for isotropic systems (e.g., sample DH-8-CN is non liquid crystalline), it should have no direct relevance to a liquid crystalline order of molecules. We can point out two possibilities to interpret this relaxation. One is the reorientation of the end to end vector of the main chain. Such a motion has been dielectrically observed for undiluted flexible polymers having dipoles aligned parallel to the chain backbone.[40,41] It is rather hard, however, to consider that our polymers, highly disordered in chemical structure, should have large enough dipoles in the backbone direction. Moreover, the dielectric relaxation associated with the end to end reorientation should be strongly molecular weight dependent, especially in undiluted systems,[40,41] and therefore we should observe a very broad distribution of relaxation time for our unfractionated, highly polydisperse systems. On the contrary, we have observed a fairly large value of b for the α' relaxation, much larger than that for the α relaxation (Table III). Thus, this possibility may be ruled out.

Another possible mode of motion may be the reorientation of the whole side chain accompanying a rotational motion of the main chain about the backbone axis. Zentel et al.,[8] who observed two dielectric relaxations above T_g for a flexible polymer having a bulky mesogenic side group, assigned the higher temperature relaxation to such a motion. The bulkiness and rigidity of the side group may be responsible for the existence of the two clearly separated relaxation processes in their system. In our system, the rigidity of the cellulose backbone may be responsible for the α' relaxation. A flexible polymer will undergo a crankshaft-like rotation over a relatively few bonds along the main chain. In a perfectly rigid rodlike molecule, the only possible rotational motion will be that of the whole molecule about the long axis. A semirigid chain like cellulose derivatives will undergo a main-chain rotation of a relatively large scale, intermediate between those of flexible and rodlike molecules. Such a large-scale motion will necessarily have a long relaxation time compared with other motions to which the α relaxation has been proposed to be assigned.

Characteristic Temperature T_s. Some words may be due regarding the "transition" T_s observed by the calorimetric analysis. Since both the α and α' relaxations are observable even below as well as above T_s, this temperature has no direct relevance to the α and α' modes of molecular motions. The DSC diagram in Figure 3 was taken at a heating rate of 10 K/min. At a smaller heating rate, say 2 K/min, both T_g and T_s remain approximately constant, but at a larger rate, T_s clearly moves toward a higher temperature, while T_g remains nearly the same (for example, T_s = 30 °C at a heating rate of 20 K/min). Moreover, no transition corresponding to T_s is observable in a cooling mode. These indicate a highly nonequilibrium nature of the "transition" T_s.

Presumably, T_s is associated with a reorganization of the molecular assembly from a less ordered state to a more ordered state. Semirigid polymers like those studied here have a tendency to order into a liquid crystal, and this tendency is stronger at lower temperatures, because the chain rigidity increases with decreasing temperature.[30] The ordering, however, is a kinetic process which requires a finite time depending on the relaxation times of molecular motions. At a low temperature slightly above T_g, where the main chain can move but extremely slowly, the ordering will require an almost infinitely long time. At a higher temperature where the relaxation times are short enough, the ordering will take place within the time scale of the experiment in question. The calorimetrically observed T_s may be understood as being this temperature. In our systems, the α' relaxation, the slower process, is perhaps a rate-determining process. Incidentally, the frequency f_{max} of the α' relaxation at T_s is on the order of 10 Hz (cf. Figure 9).

If the above discussion is correct, T_s is expected to be heating rate dependent: if the rate is too large, the ordering will not catch up with the heating process, and we will observe a broader T_s "zone" shifted toward a higher temperature. This has been observed. In a cooling process, on the other hand, we pass through a liquid crystalline state, and because this is a thermodynamically stable state, no reorganization of molecules will take place; hence, there is no transition T_s and the molecular order will be "frozen-in" at low temperatures. Solid polymer films having a liquid crystal like structure have been prepared in this manner.[42,43] Thus, it is clear that the polymer structure in the temperature region between T_g and T_s is dependent on history and, to some extent, on time. Sample DH-8-CN may appear exceptional. This sample exhibits a calorimetric transition T_s but no apparent liquid crystallinity at room temperature. On shearing, however, it readily shows strong birefringence that stands for a long time. Presumably, this sample also experiences some molecular reorganization at T_s.

Conclusion

Fully cyanoethylated DHPC exhibits three dielectric relaxations, β, α, and α'. The β relaxation is assignable to local side-chain motions. The α and α' relaxations are associated with main-chain motions that set in at T_g, of which the α mode has an activation energy about twice that of the other. It is suggested that the α' mode is associated with a rotational motion of the whole side chain about the semirigid cellulose backbone axis, while the α mode is associated with other center of mass motions of the main and side chains.

The dielectric relaxations have no direct relevance to a liquid crystalline order of molecules. The calorimetrically observed "transition" T_s may be understood as a temperature at which main-chain motions become fast enough so that the semirigid molecules can order by themselves to form a liquid crystal in the time scale of experiments.

Acknowledgment. We thank Drs. E. Kamei and S. Maeda at the Hirakata Laboratory, Ube Industries, Ltd., for kindly helping us with the dynamic viscoelastic measurements. We also thank Mr. S. Murakami at the Institute for Chemical Research, Kyoto University, for the X-ray diffraction analysis. This work was supported by a Grant-in-Aid for Scientific Research, the Ministry of Education, Japan (Grant-in-Aid 02650647).

References and Notes

(1) Seiberle, H.; Stille, W.; Strobl, G. *Macromolecules* **1990**, *23*, 2008.
(2) Kremer, F.; Vallerien, S. U.; Zentel, R.; Kapitza, H. *Macromolecules* **1989**, *22*, 4040.
(3) Attard, G. S.; Araki, K.; Moura-Ramos, J. J.; Williams, G. *Liq. Cryst.* **1988**, *3*, 861.
(4) Attard, G. S.; Araki, K.; Williams, G. *Br. Polym. J.* **1987**, *19*, 119.
(5) Bormuth, F.-J.; Haase, W. *Mol. Cryst. Liq. Cryst.* **1987**, *148*, 1; **1987**, *153*, 207.

(6) Attard, G. S.; Williams, G. *Liq. Cryst.* **1986**, *1*, 253.
(7) Attard, G. S.; Williams, G.; Gray, G. W.; Lacey, D.; Gemmel, P. A. *Polymer* **1986**, *27*, 185.
(8) Zentel, R.; Strobl, G. R.; Ringsdorf, H. *Macromolecules* **1985**, *18*, 960.
(9) Kresse, H.; Shibaev, V. P. *Macromol. Chem. Rapid Commun.* **1984**, *5*, 63.
(10) Kresse, H.; Kostromin, S.; Shibaev, V. P. *Macromol. Chem. Rapid Commun.* **1982**, *3*, 509.
(11) Kresse, H.; Talrose, R. V. *Macromol. Chem. Rapid Commun.* **1981**, *2*, 369.
(12) Gedde, U. W.; Buerger, D.; Boyd, R. H. *Macromolecules* **1987**, *20*, 988.
(13) Takase, Y.; Mitchell, G. R.; Odajima, A. *Polym. Commun.* **1986**, *27*, 76.
(14) Blundell, D. J.; Buckingham, K. A. *Polymer* **1985**, *26*, 1623.
(15) Tasaka, S.; Inagaki, N.; Miyata, S.; Chiba, T. *J. Soc. Fiber Sci. Thechnol., Jpn.* **1988**, *44*, 546.
(16) Hara, T. *Kobunshi* **1964**, *13*, 186.
(17) Morooka, T. *Wood Res.* **1987**, *74*, 45.
(18) Ishida, Y.; Yoshino, M.; Takayanagi, M.; Irie, F. *J. Appl. Polym. Sci.* **1959**, *1*, 227.
(19) Norimoto, M. *Wood Res.* **1976**, *59*, 106.
(20) Trapp, W.; Pungs, L. *Holzforschung* **1956**, *10*, 144.
(21) Nanassy, A. J. *Wood Sci. Technol.* **1970**, *4*, 104.
(22) Nishinari, K.; Shibuya, N.; Kainuma, K. *Macromol. Chem.* **1985**, *186*, 433.
(23) Abramova, E. A.; Artyukhov, A. I.; Borisova, T. I.; Bufetchikova, O. Ya. *Vysokomol. Soedin. Ser. A* **1976**, *18*, 1432.
(24) Mikhailov, G. P.; Artyukov, A. I.; Shevelev, V. A. *Vysokomol. Soedin. Ser. A* **1969**, *11*, 553.
(25) Stratton, R. A. *J. Polym. Sci., Polym. Chem. Ed.* **1973**, *11*, 535.
(26) Kimura, M.; Nakano, J. *J. Polym. Sci., Polym. Lett. Ed.* **1976**, *14*, 741.
(27) Bradley, S. A.; Carr. S. H. *J. Polym. Sci., Polym. Phys. Ed.* **1976**, *14*, 111.
(28) Nakamura, S.; Tobolsky, A. V. *J. Appl. Polym. Sci.* **1967**, *11*, 1371.
(29) Chang, Y. H.; Murakami, K. *J. Appl. Polym. Sci.* **1975**, *19*, 3015.
(30) Yamagishi, T.; Fukuda, T.; Miyamoto, T.; Watanabe, J. *Mol. Cryst. Liq. Cryst.* **1989**, *172*, 17.
(31) Yamagishi, T.; Fukuda, T.; Miyamoto, T.; Watanabe, J. *Polym. Bull.* **1988**, *20*, 373.
(32) Yamagishi, T.; Fukuda, T.; Miyamoto, T.; Watanabe, J. *Cellulose, Structural and Functional Aspects*; Kennedy, J. F., et al., Eds.; Wiley and Sons: New York, 1989; p 391.
(33) Yamagishi, T.; Fukuda, T.; Miyamoto, T.; Ichizuka, T.; Watanabe, J. *Liq. Cryst.* **1990**, *7*, 155.
(34) Yamagishi, T.; Watanabe, J.; Fukuda, T. Abstracts of IUPAC Macro 90, Montreal, Session 1.8.6, 1990.
(35) Takada, A.; Sugiura, M.; Fukuda, T.; Miyamoto, T. Abstracts of IUPAC Macro 90, Montreal, Session 1.8.6, 1990.
(36) Miyamoto, T.; Sato, T.; Kita, Y.; Inagaki, H. Abstracts of IUPAC Macro 90, Montreal, Session 1.8.6, 1990. Sato, T.; Tsujii, Y.; Kita, Y.; Miyamoto, T. Submitted for publication.
(37) According to our recent work on the anisotropic–isotropic phase transition of tri-*O*-heptylcellulose (THC), a cholesteric fraction of THC with a fairly narrow distribution in molecular weight ($M_w/M_n < 1.2$) exhibited a reasonably narrow biphasic span and a strong molecular weight dependence of T_i: it increased from 70 to 150 °C, as the molecular weight increased from 7000 to 500 000, and leveled off for higher molecular weights. An unfractionated THC with $M_w \simeq 10\,000$ and $M_w/M_n \simeq 1.8$, for example, exhibited a long biphasic region extending from about 40 to about 120 °C: Fukuda, T.; Tsujii, Y.; Takada, A.; Miyamoto, T. *Polym. Prepr. Jpn.* **1991**, *40*, 1002, 1003. The CN-DHPC samples studied here are characterized by a relatively small molecular weight (Table I) and a broad mass distribution ($M_w/M_n \simeq 2$). The wide biphasic spans exhibited by these polymers may be ascribed to the distribution in molecular weight rather than to that in chemical composition.
(38) Mikhailov, G. P. *J. Polym. Sci.* **1958**, *30*, 605.
(39) Ishida, Y.; Yamafuji, K. *Kolloid Z.* **1961**, *177*, 97.
(40) Adachi, K.; Kotaka, T. *Macromolecules* **1985**, *18*, 466.
(41) Adachi, K.; Imanishi, Y.; Kotaka, T. *J. Chem. Soc., Faraday Trans. 1*, **1989**, *85*, 1065, 1075, 1083.
(42) Watanabe, J. Personal communications.
(43) Giasson, J.; Revol, J.-F.; Gray, D. G. Abstracts of IUPAC Macro 90, Montreal, Session 1.8.6, 1990.